THE JOURNAL OF BIOLOGICAL CHEMISTRY VOL. 280, NO. 45, pp. 38020–38028, November 11, 2005

cAMP Differentially Regulates Axonal and Dendritic Development of Dentate Granule Cells*[S]

Received for publication, April 7, 2005, and in revised form, September 8, 2005 Published, JBC Papers in Press, September 9, 2005, DOI 10.1074/jbc.M503800200

Ryuji X. Yamada, Norio Matsuki, and Yuji Ikegaya[1]

From the Laboratory of Chemical Pharmacology, Graduate School of Pharmaceutical Sciences, University of Tokyo, Tokyo 113-0033, Japan

Neurite polarity is a morphological characteristic of dentate gyrus granule cells, which extend axons to the hilar region and dendrites in the opposite direction, *i.e.* to the molecular layer. This remarkable polarity must require a differential system for axon and dendrite guidance. Here, we report that the axon and dendrites of a granule cell are differentially responsive to cAMP. In developing cultures of dispersed granule cells, dendritic growth cones were increased in number after pharmacological activation of cAMP signaling and decreased after blockade of cAMP signaling. Activation of cAMP signaling antagonized dendritic collapse induced by the potent repellents Sema3F and glutamate. In contrast to dendrites, axons were protected from Sema3F-induced collapse when cAMP signaling was inhibited. Axonal and dendritic growth cones both expressed type 1 adenylyl cyclase, but only axons showed a cAMP increase in response to Sema3F, and the elevated cAMP was sufficient to collapse axonal growth cones. Thus, the axons and dendrites of dentate granule cells differ in the regulation of cAMP levels as well as responsiveness to cAMP. cAMP may be crucial for shaping the information flow polarity in the dentate gyrus circuit.

The dentate granule cells (neurons present most abundantly in the hippocampal formation) have distinctive morphology, including axodendritic polarity. They project the axons to the CA3 stratum lucidum through the dentate hilus to synapse with CA3/hilar neurons, whereas they elongate all the dendrites to the molecular layer to receive cortical synaptic inputs therein, *i.e.* the axons and dendrites are completely opposite in direction (1, 2). Such striking polarization is not found in other cortical neurons (for example, the pyramidal cells extend the axons and basal dendrites in the same direction); and therefore, they provide a unique opportunity to examine the formation of neuronal polarity.

Our previous study suggests that local environmental cues present in stratum granulosum are essential for proper neurite polarization of dentate granule cells (3), but little is known about the intracellular mechanisms. We focused this study on the influence of cAMP on the behavior of axonal and dendritic growth cones (lamellipodial structures protruding from the tips of growing neurites) because the cAMP signaling pathway is well known to modulate axonal outgrowth of various neuronal types. In *Xenopus* spinal neuron axons, netrin-1 (4) and brain-derived neurotrophic factor (5) work as attractive cues and myelin-associated glycoprotein (4) as a repulsive cue under normal conditions. However, if the intracellular cAMP level is lowered, netrin-1 and brain-derived neurotrophic factor become repulsive. If the cAMP level is increased, myelin-associated glycoprotein becomes attractive (4). Activation of cAMP signaling blocks Sema3A-mediated growth cone collapse in chick dorsal root ganglion neurons (6), but has no significant effect in *Xenopus* spinal neurons (4) and retinal neurons (7). These reports show that cyclic nucleotides modulate the neurite responses to guidance cues, but that this modulation depends on the types of guidance cues and neurons. We have demonstrated that cAMP signaling regulates pathfinding and target selection by hippocampal mossy fibers, axons of granule cells (8). However, it is unknown whether cAMP affects dendrites as well. Using dispersed cultures of granule cells, we report, for the first time, the markedly contrasting effects of cAMP on axonal and dendritic outgrowth.

The excitatory neurotransmitter glutamate regulates the dynamics of both dendritic and axonal filopodia (9–13), and accumulating evidence suggests that it also serves as a key regulator of neurite morphogenesis (14, 15). In the adult dentate gyrus, glutamate is used as a neurotransmitter at synapses from entorhinal afferents to dendrites of granule cells and from granule cell axons to CA3 pyramidal cells (16–21). Neurogenesis of granule cells, which occurs in the subgranular zone of the adult dentate gyrus, persists throughout life (22–24), and newborn neurons are functionally incorporated into mature dentate networks (25), which means that neurite guidance of granule cells also persists in adults. Therefore, it is plausible that extrasynaptic spillover of glutamate (26) from "pre-existing" synapses affects neurite pathfinding by dentate granule cells. Indeed, we have shown that glutamate mediates the guidance of mossy fiber axons (27). We thus examined whether glutamate participates in the formation of the axonal and dendritic pathways.

Finally, we examined the effect of Sema3F, a member of the family of class 3 semaphorins that have a conserved ~500-amino acid semaphorin domain at their N termini (28). Sema3F binds and activates a neuropilin-plexin receptor complex (29), in which neuropilin-2 acts as a binding subunit (30) and plexin A3 as a signal-transducing subunit (31). However, the downstream signaling of plexin A3 remains to be clarified. Sema3F is expressed in the dentate gyrus as well as in the hippocampus (32, 33) and efficiently repels axons arising from dentate gyrus tissues in collagen gel cultures (34). Sema3F seems to play a role in stereotyped pruning of infrapyramidal mossy fibers, as assessed in mutant mice lacking Sema3F, neuropilin-2, and plexin A3 (34–36). However, no studies have addressed the effect of Sema3F on dendritic outgrowth. We report that Sema3F collapses growth cones of axons and dendrites with a similar potency, but we also found that cAMP contributes differentially to Sema3F signaling in axonal and dendritic responses. Such contrasting actions of cAMP could underlie the opposing extension of axons and dendrites of dentate granule cells.

* This work was supported in part by a grant-in-aid for scientific research from the Ministry of Education, Culture, Sports, Science, and Technology of Japan. The costs of publication of this article were defrayed in part by the payment of page charges. This article must therefore be hereby marked "*advertisement*" in accordance with 18 U.S.C. Section 1734 solely to indicate this fact.

[S] The on-line version of this article (available at http://www.jbc.org) contains supplemental Fig. 1.

[1] To whom correspondence should be addressed: Lab. of Chemical Pharmacology, Graduate School of Pharmaceutical Sciences, University of Tokyo, 7-3-1 Hongo, Bunkyo-ku, Tokyo 113-0033, Japan. Tel.: 81-3-5841-4783; Fax: 81-3-5841-4786; E-mail: ikegaya@mol.f.u-tokyo.ac.jp.

MATERIALS AND METHODS

Pharmacological Agents—Forskolin, SQ 22,536 (9-(tetrahydro-2-furanyl)-9*H*-purin-6-amine), and KT 5720 were purchased from Sigma. 8-Bromo (8-Br)[2]-cAMP (sodium salt) and myristoylated protein kinase A (PKA) inhibitor (PKI)-(14–22)-amide were obtained from Calbiochem. (1*S*,3*R*)-1-Aminocyclopentane-1,3-dicarboxylic acid (ACPD) and (*RS*)-α-methyl-4-carboxyphenylglycine (MCPG) were from Tocris Cookson (Bristol, UK).

Dispersed Cultures of Granule Cells—Postnatal day 3 Wistar/ST rats (Japan SLC, Inc., Shizuoka, Japan) were deeply anesthetized by hypothermia, and the hippocampal formation was dissected out and placed in ice-cold Gey's balanced salt solution. After removal of the subicular complex and the Ammon horn, the remaining part, *i.e.* the dentate gyrus, was trypsinized and gently triturated. Isolated cells were plated at a density of 5.0×10^3 cells/cm^2 onto 13-mm coverslips coated with poly-L-lysine (Sigma) and cultivated in 50% Neurobasal/B-27 medium (Invitrogen) and 50% astrocyte-conditioned medium (8) at 37 °C in a humidified 5% CO_2 and 95% air atmosphere. The culture medium was changed to conditioned medium-free Neurobasal/B-27 medium supplemented with 2 μM cytosine D-arabinofuranoside (Sigma) 24 and 72 h after plating. These procedures consistently allowed us to prepare granule cell cultures with high purity (>75%) (3, 37, 38).

Conditioned Medium from Sema3F-transfected COS-7 Cells—pEF-Sema3F-Myc (mouse) and pEF-Myc (control) were provided by Dr. Atsushi Tamada (National Institute for Basic Biology, Okazaki, Japan). The COS-7 cells were maintained in Dulbecco's modified Eagle's medium (Nacalai Tesque, Inc., Kyoto, Japan) supplemented with 10% fetal bovine serum, 50 units/ml penicillin G, and 100 μg/ml streptomycin. The medium was changed to serum-free Dulbecco's modified Eagle's medium 24 h after plating. Transfection into cells was performed with FuGENE 6 (Roche Applied Science) according to the manufacturer's instructions. After another 72 h, the supernatants obtained by centrifugation at $100 \times g$ for 5 min at 4 °C were collected and stored at −80 °C after filtration through filters with a 0.20-μm pore size. Once thawed, the conditioned medium was used within 12 h. For every preparation, Sema3F-Myc content was confirmed by Western blot analysis with anti-Myc antibody (see below), which revealed that almost the same amount of Sema3F was consistently obtained in the conditioned medium. Unless specified otherwise, the medium was used at a 1:32 dilution in assays. Preliminary experiments showed that a 10-min treatment with the Sema3F-containing medium caused a 75% decrease in sympathetic neuron growth cones prepared from embryonic day 17–18 Wistar/ST rats compared with the control medium, indicating that the expressed Sema3F-Myc was functional (data not shown).

Growth Cone Collapse Assay—Treatment with drugs was carried out at 37 °C in a humidified 5% CO_2 and 95% air atmosphere. Four days after plating, primary cultures of dentate granule cells were treated with glutamate or ACPD together with MCPG or 8-Br-cAMP for 30 min and immediately fixed to perform immunocytochemical analysis. To test the effect of Sema3F, cells were pretreated with cAMP-related reagents or peptides, including forskolin (20 min), 8-Br-cAMP (30 min), KT 5720 (40 min), SQ 22,536 (30 min), and myristoylated PKI (60 min), and subsequently treated with conditioned medium prepared from Sema3F-transfected COS-7 cells (10 min) in the presence of the same drugs or peptides. To evaluate the synergic effect of forskolin and Sema3F, we treated cells with either or both of them for 10 min. In some experiments, cultures were maintained in the control conditioned medium for 10 min before fixation. The cultures were treated for 20 min at 37 °C with fixative consisting of 4% paraformaldehyde, 0.25% glutaraldehyde (Nacalai Tesque, Inc.), 0.1% Triton X-100, 10 μM Taxol (Sigma), and 1.3 μM phalloidin (Sigma) in 60 mM PIPES, 25 mM HEPES, 10 mM EGTA, and 2 mM $MgCl_2$ (pH 6.9) (39).

Quantification of Growth Cones—Fixed cultures were treated with 2% goat serum for 60 min and overnight at 4 °C with mouse anti-tau-1 monoclonal (1:2000 dilution; catalog no. MAB3420, Chemicon International, Inc., Temecula, CA) and rabbit anti-microtubule-associated protein-2 (MAP-2; 1:1000 dilution; catalog no. AB5622, Chemicon International, Inc.) primary antibodies. They were then treated with Alexa 488-labeled anti-mouse IgG (1:400 dilution; catalog no. A-11001, Molecular Probes, Inc.) and Alexa 350-labeled anti-rabbit IgG (1:400 dilution; catalog no. A-11046, Molecular Probes, Inc.) secondary antibodies in the presence of rhodamine-conjugated phalloidin (1:40 dilution; catalog no. R415, Molecular Probes, Inc.) for 5 h at room temperature. Immunohistological images were acquired with a Hamamatsu ORCA II cooled CCD camera and a ×40 objective equipped with a Nikon Eclipse TE300 inverted microscope and analyzed with an AquaCosmos system (Hamamatsu Photonics, Hamamatsu, Japan). We selected cells that were spatially isolated from other cells and that had round (granule-like) somata: one tau-1-positive and MAP-2-negative neurite (referred here to as an axon) and some tau-1-negative and MAP-2-positive neurites (dendrites) (40, 41). According to these criteria, ~57% of the cells were discarded before data analysis. Phalloidin specifically detects F-actin, which is expressed in a large amount in growth cones, so we defined the growth cone as a phalloidin-positive protrusion with at least 10 μm^2 of lamellipodia and visible filopodia (42, 43). For dendritic protrusions, we counted only growth cones that did not overlap neighboring protrusions. For each neuron, collapsed and uncollapsed growth cones were counted, and the data are presented as the percentage of collapsed growth cones to the total number of protrusions. The numbers of cells and experiments are given in the figure legends.

Immunocytochemistry for Adenylyl Cyclase—Cultures were fixed with 4% paraformaldehyde for 30 min at 37 °C, permeabilized with 0.1% Triton X-100 for 30 min, and blocked with 2% goat serum for 60 min. They were treated overnight at 4 °C with the primary antibodies against tau-1 (1:2000 dilution) and rabbit pan adenylyl cyclase (1:400 dilution; catalog no. sc-1701, Santa Cruz Biotechnology, Inc., Santa Cruz, CA) or rabbit type 1 adenylyl cyclase (1:400 dilution; catalog no. sc-586, Santa Cruz Biotechnology, Inc.) and then with Alexa 350-labeled anti-mouse IgG (1:400 dilution) and Alexa 488-labeled anti-rabbit IgG (1:400 dilution) secondary antibodies in the presence of rhodamine-conjugated phalloidin (1:40 dilution) for 3 h at room temperature. Fluorescent images were collected as described above.

cAMP Immunoassay—We adopted the methods introduced by Chemicon International, Inc., as described previously (44). After 4 days in culture, cells were treated with the control medium, forskolin (100 μM forskolin + control medium), or Sema3F (Sema3F-containing medium); fixed with 4% paraformaldehyde for 30 min at 37 °C; and permeabilized with 0.4% Triton X-100 containing 3% goat serum for 30 min. They were incubated with anti-tau-1 (1:2000 dilution) and rabbit anti-cAMP (1:1000 dilution; catalog no. AB306, Chemicon International, Inc.) primary antibodies in the presence of 1% goat serum for 2 h at room temperature, incubated overnight at 4 °C, and then incubated with Alexa 350-labeled anti-mouse IgG (1:400 dilution) and Alexa 488-labeled anti-rabbit IgG (1:400 dilution) secondary antibodies in the presence of rhodamine-conjugated phalloidin (1:40 dilution) for 3 h at

[2] The abbreviations used are: 8-Br, 8-bromo; PKA, protein kinase A; PKI, protein kinase A inhibitor; ACPD, (1*S*,3*R*)-1-aminocyclopentane-1,3-dicarboxylic acid; MCPG, (*RS*)-α-methyl-4-carboxyphenylglycine; PIPES, 1,4-piperazinediethanesulfonic acid; MAP-2, microtubule-associated protein-2; ANOVA, analysis of variance.

room temperature. Fluorescent images were collected as described above.

Digital Quantification of Fluorescence Intensity in Growth Cones—The contour of a growth cone was manually traced on its rhodamine-conjugated phalloidin image. The fluorescence intensity of anti-adenylyl cyclase and anti-cAMP antibodies was measured within the contour and normalized to unit area. For each growth cone, the background fluorescence was obtained from three adjacent 4×4-μm^2 areas, which were >1 μm apart from the growth cone and positioned in the 0°, 90°, and 270° angles from the growth cone stem axis. These three background values were averaged, and the immunosignal is expressed as (growth cone value − background level)/background level.

Measurement of Area and Volume of Growth Cones—Four days after plating, primary cultures of granule cells were incubated with prewarmed (37 °C) Neurobasal/B-27 medium containing 10 μM CellTracker Green (5-chloromethylfluorescein diacetate; Molecular Probes, Inc.). After 30 min at 37 °C, the medium was replaced with fresh prewarmed medium, and cells were incubated for an additional 30 min at 37 °C. Cells were immediately washed with phosphate-buffered saline and fixed with 4% paraformaldehyde for 30 min at 37 °C, permeabilized with 0.4% Triton X-100, and then incubated with rhodamine-conjugated phalloidin (1:40 dilution) for 3 h at room temperature. Each growth cone was analyzed three-dimensionally with a *z* axis interval of 0.5 μm using a Bio-Rad MRC-1024 confocal system with a ×60 objective. CellTracker-positive areas in confocal *xy* planes were integrated across the *z* axis and calculated as the volume of the growth cone. Phalloidin-positive areas in the same field were stacked in a single layer and calculated as the areas of the growth cones. As a result, we found that the volume of the growth cone was linearly correlated with the area, presumably because the thickness of the lamellipodia was almost even in the space of a culture plate. Therefore, the growth cone volume can be replaced with its phalloidin-positive area, a parameter that is easy to record, to evaluate the cAMP concentration in the growth cone (see above).

Sema3F Pre-absorption—Protein G-Sepharose (12.5 μl; Amersham Biosciences, Buckinghamshire, UK) was incubated with 12.5 μg of a monoclonal antibody (9E10) against a C-terminal Myc epitope tag (45) in immunoprecipitation buffer consisting of 50 mM Tris-HCl (pH 7.4) and 150 mM NaCl at 4 °C for 2 h. The beads were washed two times with 50 μl of immunoprecipitation buffer and three times with 200 μl of Dulbecco's modified Eagle's medium and then incubated with 600 μl of Sema3F-conditioned medium or control medium at 4 °C for 2 h, and the supernatants were harvested as absorbed Sema3F or absorbed control, respectively. As a control without antibody (non-absorbed Sema3F), the beads were incubated with 25 μl of immunoprecipitation buffer (instead of the antibody) for 2 h and then with 600 μl of Sema3F-conditioned medium for 2 h after washing.

Western Blot Analysis—The conditioned medium from COS-7 cells was separated by SDS-PAGE and transferred onto polyvinylidene difluoride membranes. The membranes were incubated at room temperature for 1 h in phosphate-buffered saline containing 0.05% Tween 20 and 5% skimmed milk and then treated overnight with anti-Myc antibody (1:1000 dilution) at 4 °C. The membranes were washed for 15 min and incubated with peroxidase-conjugated anti-mouse IgG antibody (1:1000 dilution) for 1 h at room temperature. Proteins bound to the antibody were visualized with an ECL Plus enhanced chemiluminescence kit (Amersham Biosciences). Anti-Myc antibody specifically detected one band with a molecular mass of ~88.5 kDa, which corresponds to the combined size of Sema3F and c-Myc.

Data Analysis and Statistics—Imaging and quantification were performed by two independent people in a blind manner to avoid bias. Data are expressed as means ± S.E. and were statistically analyzed with one-way repeated-measures analysis of variance (ANOVA) and post-hoc Tukey's test for multiple pairwise comparisons.

RESULTS

Granule cells were prepared from postnatal rat dentate gyri and used in experiments at day 4 in culture when each neuron consistently developed the longest tau-1-positive neurite and several tau-1-negative neurites (Fig. 1*A*) (40). The tau-1-positive neurites were always MAP-2-negative, whereas other tau-1-negative neurites were MAP-2-positive (data not shown) (46). Therefore, we considered the tau-1-positive neurites as growing axons and the other shorter ones as growing dendrites. We regarded growth cones as "uncollapsed" protrusions from neurites; specifically, they were defined as phalloidin-positive lamellipodia (>10 μm^2) with few visible filopodia. On average, individual neurons extended one axon and 5.1 ± 0.1 dendrites and bore 4.0 ± 0.3 protrusions from the axons and 7.7 ± 0.3 protrusions from the dendrites per cell, out of which 38.21 ± 3.29% (axons) and 35.88 ± 2.16% (dendrites) formed growth cones under basal conditions ($n = 86$ cells).

cAMP Protects Dendritic Growth Cones against Metabotropic Glutamate Receptor Activation-induced Collapse—We have previously shown that the neurotransmitter glutamate regulates guidance of hippocampal mossy fibers in hippocampal slice cultures (27). In a first series of experiments, we therefore sought to determine how glutamate affects the behavior of growth cones of axons and dendrites.

We treated granule cell cultures with 50 μM glutamate for 30 min. This induced a decrease in the number of both axonal and dendritic growth cones (Fig. 1, *A* and *B*). Glutamate-induced collapse of dendritic growth cones was prevented by 300 μM MCPG (47), an antagonist of group I/II metabotropic glutamate receptors, whereas this antagonist was ineffective in axons (Fig. 1, *A* and *B*). 6-Cyano-7-nitroquinoxaline-2,3-dione (10 μM), an antagonist of non-*N*-methyl D-aspartate glutamate receptors, completely blocked axonal collapse (data not shown). Neither MCPG nor 6-cyano-7-nitroquinoxaline-2,3-dione alone affected growth cones of axons or dendrites (Fig. 1*B*) (data not shown). Thus, glutamate recruits different intracellular mechanisms in axons and dendrites. This notion was supported by a differential action of ACPD (47), an agonist of group I/II metabotropic glutamate receptors; ACPD induced growth cone collapse only in dendrites (Fig. 1, *A* and *C*).

Group II metabotropic glutamate receptors are linked to inhibition of cAMP signaling via $G_{i/o}$ protein activation (47). Consistent with this, 300 μM 8-Br-cAMP (48), a membrane-permeable analog of cAMP, canceled ACPD-induced collapse of dendritic growth cones (Fig. 1, *A* and *C*). Interestingly, blockade of cAMP signaling by a 40-min treatment with the adenylyl cyclase inhibitor SQ 22,536 (49) alone led to growth cone collapse in dendrites (Fig. 2*A*). A similar effect was obtained with KT 5720 (50, 51), an inhibitor of PKA (Fig. 2*B*). To examine whether blockade of cAMP/PKA signaling induces growth cone collapse as well as changes the number or morphology of neurites, we simultaneously monitored the length of axons, the number of primary dendrites, and the number of terminal protrusions per axon and dendrite (TABLE ONE). None of these parameters was unaffected by the cAMP/PKA inhibitors. Therefore, inhibition of the cAMP/PKA pathway is sufficient to collapse dendritic growth cones; in other words, dendritic growth cones are maintained by constitutive activation of cAMP/PKA signaling. On the other hand, neither SQ 22,536 nor KT 5720 affected axonal growth cones (Fig. 2).

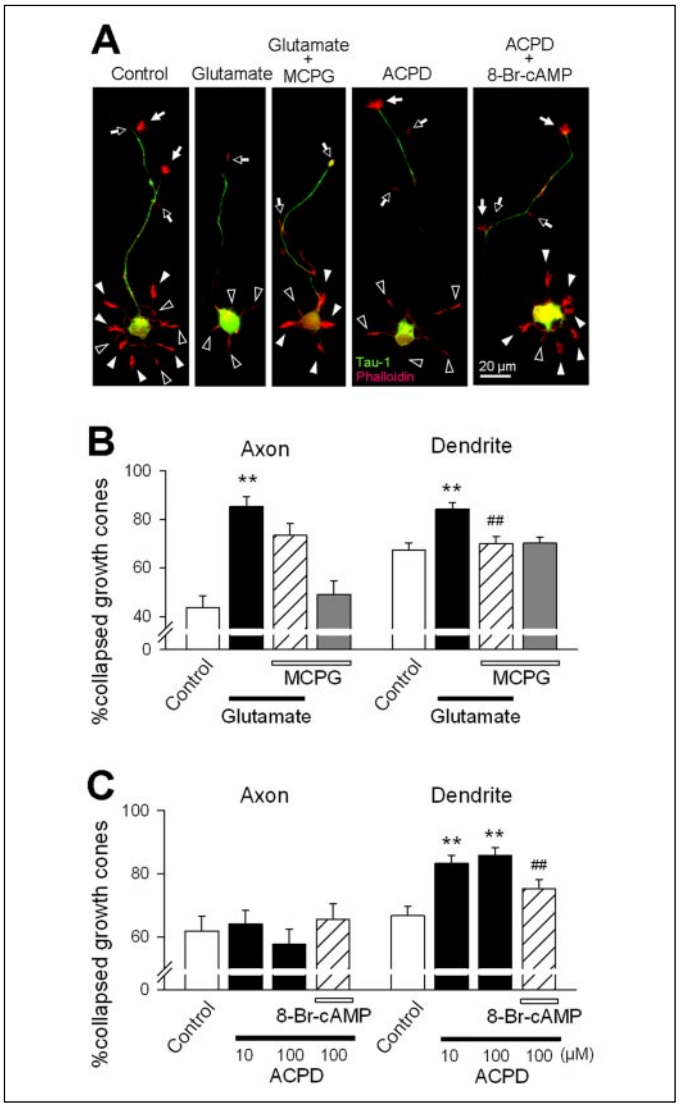

FIGURE 1. **Activation of cAMP signaling prevents group I/II metabotropic glutamate receptor-induced collapse of dendritic growth cones of dentate granule cells.** *A*, epifluorescent images of cultured granule cells co-stained with rhodamine-conjugated phalloidin (*red*) and anti-tau-1 antibody (*green*) 30 min after treatment with combinations of 50 μM glutamate, 300 μM MCPG (an antagonist of group I/II metabotropic glutamate receptors), 100 μM ACPD (an agonist), and 300 μM 8-Br-cAMP (a cAMP analog). We defined the axon as the longest tau-1-positive neurite and dendrites as the other tau-1-negative neurites and counted their phalloidin-positive growth cones (see "Materials and Methods"). *Closed arrows* and *arrowheads* indicate intact (uncollapsed) growth cones of axons and dendrites, respectively. *Open arrows* and *arrowheads* indicate "collapsed" growth cones of axons and dendrites, respectively. For our definition of collapsed/uncollapsed growth cones, see "Materials and Methods." *B*, treatment with 300 μM MCPG rescues 50 μM glutamate-induced collapse of dendrites, but not of axons (*hatched bars*). The *ordinate* indicates the percentage of collapsed growth cones to the total number of protrusions. *C*, activation of cAMP signaling prevents ACPD-induced collapse of dendritic growth cones. ACPD caused growth cone collapse of dendrites in a concentration-dependent manner, but failed to affect axonal growth cones (*black bars*). This effect was significantly (although partially) blocked by co-treatment with 300 μM 8-Br-cAMP (*hatched bars*). The values given by the *white* and *hatched bars* are not significantly different. Growth cones were counted after a 30-min exposure to glutamate or ACPD. Data represent means ± S.E. of 49–54 neurons obtained from five independent experiments (*B*) and 59–65 neurons from six experiments (*C*). **, $p < 0.01$ *versus* control; ##, $p < 0.01$ *versus* glutamate or 100 μM ACPD (Tukey's test after ANOVA).

cAMP Differentially Regulates Axonal and Dendritic Outgrowth of Granule Cells—In addition to the above results, our previous *ex vivo* study shows that the cAMP signaling pathway plays a role in proper target selection by the axons of dentate granule cells (8). We therefore focused the remaining part of this work on the involvement of cAMP signaling in axonal and dendritic outgrowth of granule cells.

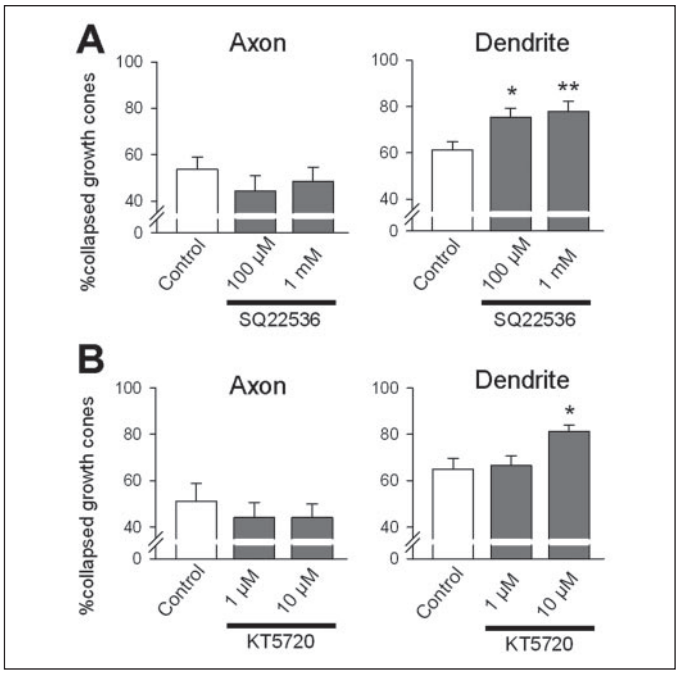

FIGURE 2. **Constitutive activation of the cAMP signaling pathway is required for maintenance of dendritic (but not axonal) growth cones of dentate granule cells.** Granule cells were treated with the adenylyl cyclase inhibitor SQ 22,536 for 30 min (*A*) or the PKA inhibitor KT 5720 for 40 min (*B*) at the concentrations indicated and then with the control medium for another 10 min in the presence of these drugs, and the responses of growth cones were quantified. Data represent means ± S.E. of 40–52 neurons from five independent experiments (*A*) and 30–39 neurons from four experiments (*B*). *, $p < 0.05$ *versus* control; **, $p < 0.01$ *versus* control (Turkey's test after ANOVA).

TABLE ONE

Morphometric analysis of dentate granule cells (inhibition of cAMP signaling)

Data are mean ± S.E.

Reagents	Axon		Dendrite	
	Length	No. of terminals	No. of primary dendrites	No. of terminals
	μm			
SQ 22,536				
Control	122.22 ± 5.91	2.54 ± 0.19	6.63 ± 0.31	7.15 ± 0.35
100 μM	127.20 ± 4.95	2.63 ± 0.28	6.39 ± 0.30	6.83 ± 0.35
1 mM	118.34 ± 5.42	2.16 ± 0.19	6.28 ± 0.27	6.88 ± 0.42
KT 5720				
Control	122.04 ± 11.45	2.17 ± 0.24	5.49 ± 0.23	6.73 ± 0.28
1 μM	118.25 ± 7.93	2.53 ± 0.23	5.32 ± 0.25	7.67 ± 0.35
10 μM	111.67 ± 5.60	2.41 ± 0.23	5.23 ± 0.29	7.05 ± 0.35

Granule cell cultures were treated for 30 min with forskolin (52), an activator of adenylyl cyclase. Surprisingly, forskolin exerted contrasting effects on axons and dendrites; it decreased the number of growth cones in axons, but increased the number of dendritic growth cones (Fig. 3*A*). These results were replicated by a 40-min treatment with 8-Br-cAMP (Fig. 3*B*). We analyzed the effect of these cAMP/PKA activators on neurite morphology (TABLE TWO), but we did not find any significant effect. These results indicate, for example, that the increase in dendritic growth cones shown in Fig. 3 was not attributable to an increase in the total number of dendrites per cell. Therefore, cAMP signaling differentially modulates the behavior of axonal and dendritic growth cones.

What brought about such a striking difference? We carried out immunostaining with anti-pan adenylyl cyclase antibody to examine the subcellular distribution of this cAMP-producing enzyme. Growth

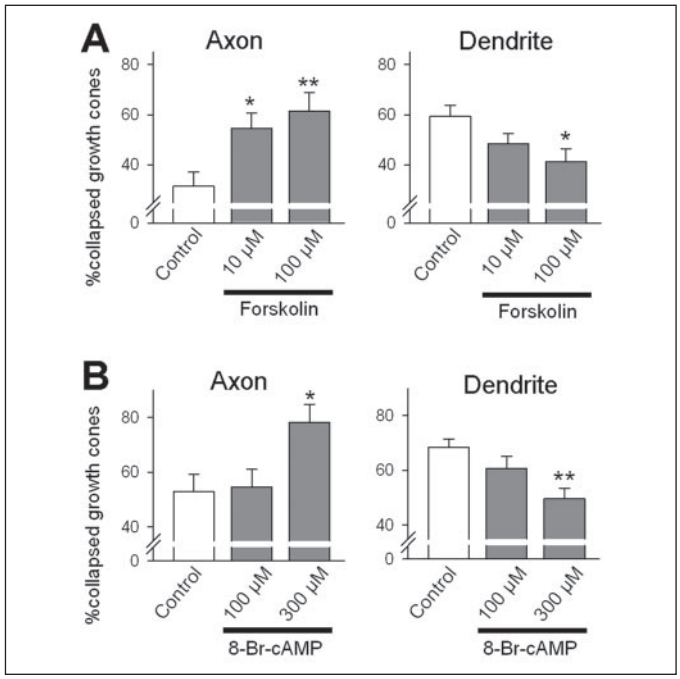

FIGURE 3. **Opposite responses of axonal and dendritic growth cones to cAMP stimulation.** Granule cell cultures at day 4 *in vitro* were treated with or without the adenylyl cyclase activator forskolin for 20 min (*A*) or 8-Br-cAMP for 30 min (*B*) and then with the control medium for another 10 min. Data represent means ± S.E. of 31–48 neurons from six independent experiments (*A*) and 24–38 neurons from four experiments (*B*). *, $p < 0.05$ *versus* control; **, $p < 0.01$ *versus* control (Tukey's test after ANOVA).

TABLE TWO

Morphometric analysis of dentate granule cells (activation of cAMP signaling)

Data are mean ± S.E.

Reagents	Axon		Dendrite	
	Length	No. of terminals	No. of primary dendrites	No. of terminals
	μm			
Forskolin				
Control	135.70 ± 10.35	3.14 ± 0.27	5.67 ± 0.33	6.14 ± 0.37
10 μM	135.45 ± 6.23	3.02 ± 0.23	5.24 ± 0.24	5.81 ± 0.26
100 μM	137.69 ± 8.32	3.61 ± 0.35	5.31 ± 0.24	5.45 ± 0.26
8-Br-cAMP				
Control	113.67 ± 4.96	2.47 ± 0.25	6.05 ± 0.34	7.58 ± 0.36
100 μM	118.87 ± 6.23	2.19 ± 0.16	6.51 ± 0.28	6.78 ± 0.31
300 μM	127.26 ± 9.71	2.5 ± 0.28	6.40 ± 0.44	7.08 ± 0.36

cones of granule cells expressed adenylyl cyclase in the neck and lamellipodial domain, but we found no evidence for a significant difference in the spatial pattern or level of immunoreactivity between axons and dendrites (Fig. 4, *A* and *B*). Of the known adenylyl cyclases, type 1 adenylyl cyclase is present in the dentate gyrus with the highest mRNA expression (53, 54), and mutant mice lacking this gene show reduced synaptic potentiation of the granule cell axons (55). We therefore examined the immunoreactivity for type 1 adenylyl cyclase in growth cones, and we again found no difference in its expression between axons and dendrites (Fig. 4*C*).

We next measured the cellular level of cAMP to determine whether the adenylyl cyclases present in growth cones are functional. We used an antibody that binds to free cAMP in the cytosol (44). Granule cells were labeled with anti-cAMP antibody after a 5-min exposure to 100 μM forskolin. Forskolin induced a 30–40% increase in the cAMP immunoreactivity in both axonal and dendritic growth cones (Fig. 5*B*). Therefore, the axodendritic difference, *i.e.* forskolin-induced decrease/increase in the number of axonal/dendritic growth cones, is unlikely attributable to the cAMP production system.

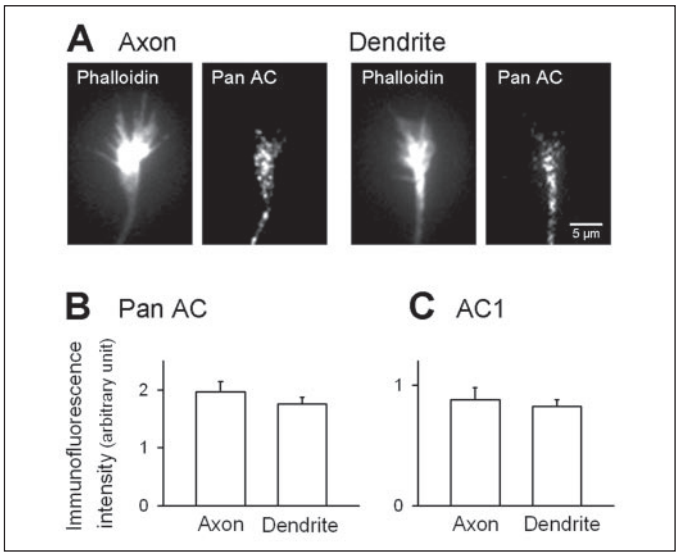

FIGURE 4. **Dentate granule cells express adenylyl cyclase in both axonal and dendritic growth cones.** *A*, microscopic fluorescent images of axonal (*left panels*) and dendritic (*right panels*) growth cones stained with rhodamine-conjugated phalloidin and anti-pan adenylyl cyclase antibody (*Pan AC*) at day 4 *in vitro*. Each pair of images was obtained from the same microscopic field. *B* and *C*, no difference in immunofluorescent reactivity against anti-pan adenylyl cyclase antibody or anti-type 1 adenylyl cyclase antibody (*AC1*), respectively, in axons and dendrites ($p > 0.5$, Student's *t* test; see "Materials and Methods"). Data represent means ± S.E. of 41 (*B*) and 22 (*C*) axonal growth cones and 69 (*B*) and 50 (*C*) dendritic growth cones from three independent experiments.

Sema3F Collapses Growth Cones of Both Axons and Dendrites of Granule Cells—Sema3F is expressed in the hippocampal formation including the dentate gyrus (32) and works as a potent repellent against mossy fiber axons (34, 35, 36), yet the effect of Sema3F on dendritic outgrowth has not been examined, and the intracellular mechanisms for neurite repulsion have not been fully elucidated. We treated granule cells for 10 min with the culture medium harvested from COS-7 cells transfected with Myc-tagged *Sema3F* cDNA. Sema3F-Myc was readily secreted in the medium because anti-Myc antibody detected a band with a molecular mass of ~88.5 kDa, consistent with the total size of Sema3F and c-Myc (Fig. 5*D*, *inset*). To depict a concentration-response curve, we diluted the medium in the range of 1:256 to 1:16. The medium collapsed growth cones of both axons and dendrites (Figs. 6 and 7), and the potency was almost equivalent between them (Fig. 6*A*). In the following experiments, we used a 1:32 dilution of the culture medium.

In control experiments, we carefully used the media obtained from sister cultures transfected with the corresponding control vector, but we still desired to verify that Sema3F medium-induced growth cone collapse was due to the action of Sema3F protein rather than other molecules present in the medium. For this purpose, we reduced the level of Myc-tagged Sema3F in the conditioned medium by immunoprecipitation with anti-Myc antibody (Fig. 5*D*, *inset*). We confirmed that this pre-absorbed supernatant did not collapse axonal or dendritic growth cones any longer, although the supernatant prepared following the same procedures without anti-Myc antibody (non-absorbed Sema3F) was still effective (Fig. 6*B*). We thus concluded that Sema3F protein was responsible for the collapsing activity of the medium.

cAMP Mediates Sema3F-induced Growth Cone Collapse of Axons, but Not of Dendrites—We sought to determine whether Sema3F alters the level of cAMP in growth cones. Granule cell cultures were exposed

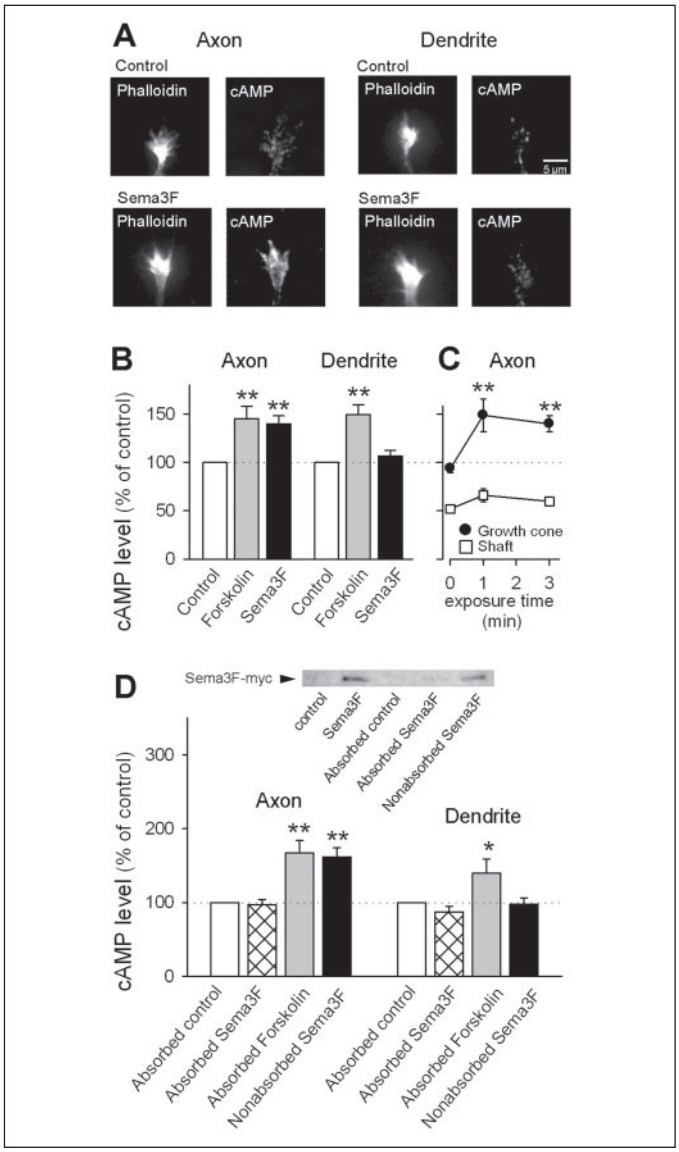

FIGURE 5. **Forskolin and Sema3F differentially influence cAMP levels in growth cones of dentate granule cells.** *A*, anti-cAMP immunoreactivity in axonal and dendritic growth cones stained with phalloidin at day 4 *in vitro*. Axons were determined based on tau-1 immunoreactivity. Cultures were treated with the control medium (*upper panels*) or Sema3F-containing medium (*lower panels*) for 180 s. Each image pair was obtained from the same field. These media were used at a 1:32 dilution (see Fig. 6*A*). *B*, quantification of cAMP immunoreactivity in growth cones treated with the control medium for 3 min (*open bars*), forskolin for 5 min (*gray bars*), or Myc-tagged Sema3F-containing medium for 3 min (*black bars*) at day 4 *in vitro*. Forskolin was dissolved in the control medium. The Sema3F-containing medium increased cAMP levels in growth cones of axons, but not of dendrites, whereas forskolin increased cAMP levels in growth cones of both axons and dendrites. Data represent means ± S.E. of 23–37 growth cones from three independent experiments. **, $p < 0.01$ *versus* control (Tukey's test after ANOVA). *C*, time course of changes in the cAMP level in axonal growth cones after Sema3F treatment. The cAMP immunoreactivity in axons was assessed in growth cones (●) and shafts (□). cAMP levels are expressed as a percentage of the value of growth cones in the control supernatant-treated group at each time point (see "Materials and Methods"). Axonal growth cones displayed higher cAMP levels compared with shafts and an additional cAMP increase in response to Sema3F, and this effect lasted for 3 min, whereas no apparent change was found in axonal shafts. Data represent means ± S.E. of 17–37 growth cones and 20–30 shafts from three experiments. **, $p < 0.01$ *versus* growth cones at 0 min (Tukey's test after ANOVA). *D*, pre-absorption with anti-Myc antibody blocks the cAMP elevation induced by Sema3F-containing medium, but not by forskolin. The Sema3F-containing medium that did not receive treatment with anti-Myc antibody (non-absorbed Sema3F) was used as a positive control (*black bars*). The control and Sema3F-containing media treated with the antibody are referred to as absorbed control (*white bars*) and absorbed Sema3F (*cross-hatched bars*), respectively. Western blotting (*inset*) confirmed that our pre-absorption procedure substantially reduced the level of Sema3F protein in the conditioned medium obtained from COS-7 cultures transfected with Myc-tagged Sema3F. The band detected at the expected molecular mass (~88.5 kDa) is shown here as Sema3F. Forskolin was dissolved in the absorbed control medium (absorbed forskolin) (*gray bars*). Data represent means ± S.E. of 10–25 growth cones from four independent experiments. *, $p < 0.05$ *versus* absorbed control; **, $p < 0.01$ *versus* absorbed control (Tukey's test after ANOVA).

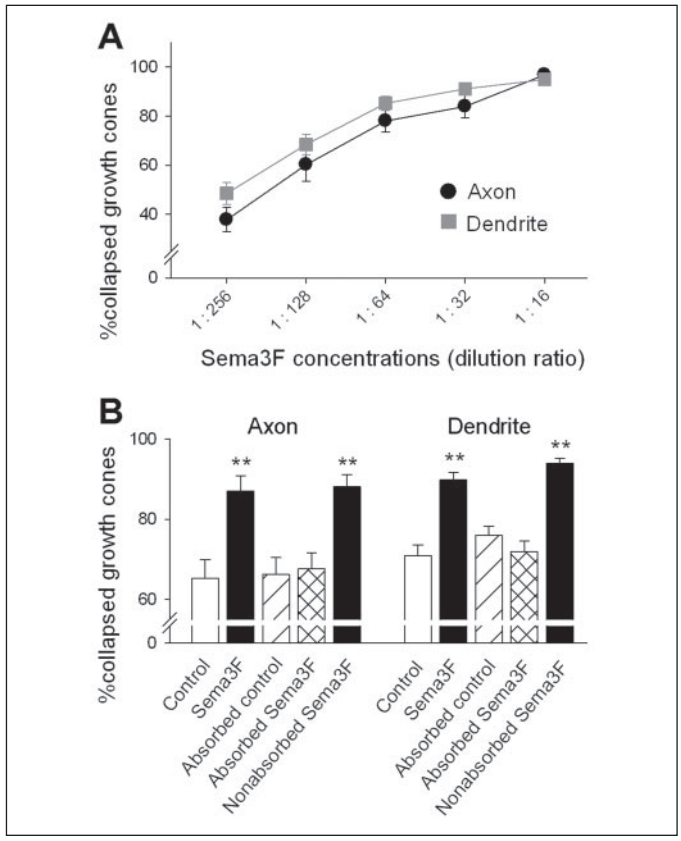

FIGURE 6. **Sema3F induces growth cone collapse in axons and dendrites with a similar dose dependence.** *A*, response curves for axonal (*black circles*) and dendritic (*gray squares*) growth cone collapse of dentate granule cells as a function of the dilution ratio of the Sema3F supernatant. The effect of the Sema3F supernatant was evaluated after a 10-min treatment. In the following experiments, the Sema3F supernatant was used at a 1:32 dilution. Data represent means ± S.E. of 32–51 neurons from five independent experiments. *B*, pre-absorption with anti-Myc antibody abolishes growth cone collapse. The results confirm that the effect of the Sema3F supernatant was mediated by Sema3F itself, but not by other concomitants (for details, see Fig. 5 and "Materials and Methods"). Data represent means ± S.E. of 58–79 neurons from five independent experiments. **, $p < 0.01$ *versus* control (Tukey's test after ANOVA).

to the control or Sema3F-containing medium for 3 min and immediately fixed and processed for anti-cAMP immunostaining. The Sema3F-containing medium induced a cAMP increase in axons, but in not dendrites (Fig. 5, *A* and *B*). Pre-absorption with anti-Myc antibody excluded this action of the medium containing Myc-tagged Sema3F but not forskolin (Fig. 5*D*). To evaluate the time course of changes in the cAMP levels in axonal growth cones, we stimulated cells with Sema3F, followed by analysis at various time points. The cAMP level was already elevated after 1 min and was maintained for at least 3 min (Fig. 5*C*), although we could not quantify the cAMP level for a longer time because Sema3F collapses growth cones. The base-line cAMP immunofluorescence intensity was lower in axonal shafts compared with growth cones, and no apparent change in cAMP levels was observed after Sema3F treatment (Fig. 5*C*). These data indicate that a rise in cAMP levels in axonal growth cones precedes Sema3F-induced axonal collapse.

To address whether this cAMP increase is linked to growth cone collapse, we applied SQ 22,536 for 30 min and subsequently together with Sema3F for 10 min. In the presence of SQ 22,536 at a high concen-

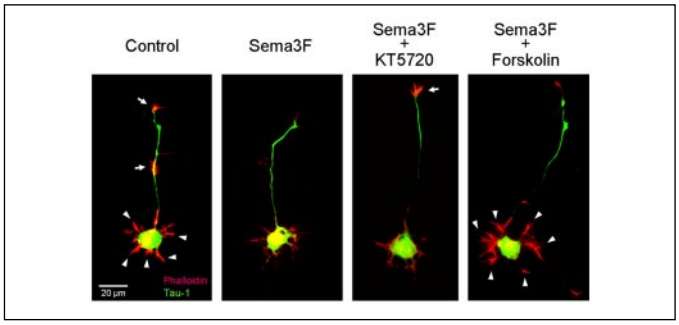

FIGURE 7. **cAMP signaling mediates Sema3F-induced collapse of axonal growth cones and prevents Sema3F-induced dendritic collapse.** Shown are typical microscopic fluorescent images of isolated granule cells stained with rhodamine-conjugated phalloidin (*red*) and anti-tau-1 antibody (*green*) after a 10-min treatment with the control supernatant (*first panel*) or the Sema3F-containing supernatant in the absence (*second panel*) and presence of 10 μM KT 5720 (*third panel*) or 100 μM forskolin (*fourth panel*). *Arrows* and *arrowheads* indicate uncollapsed growth cones of axons and dendrites, respectively. Data are summarized in Figs. 8 and 9.

tration (1 mM), Sema3F did not collapse axonal growth cones (Fig. 8*A*). Similar results were obtained with KT 5720 pretreatment (Figs. 7 and 8*B*). In general, pharmacological agents might not behave in a specific manner, in particular, if they are used at high concentrations. We therefore used a cell-permeable myristoylated PKA pseudo-substrate peptide (PKI) as a reliable, highly specific PKA inhibitor (Fig. 8*C*) (56). We confirmed that PKI also prevented Sema3F-induced axonal collapse. Activation of cAMP signaling by pretreatment with forskolin for 20 min (Figs. 7 and 9A) or 8-Br-cAMP for 30 min (Fig. 9*B*) did not affect the action of Sema3F, *i.e.* high concentrations of these reagents did not enhance the collapse induced by Sema3F. At subsaturating concentrations of Sema3F (1:128 dilution) and forskolin (3 μM), these two reagents were synergic; stimulation with either alone did not induce any collapse responses, but co-application did (Fig. 8*D*). Therefore, cAMP/PKA signaling likely to mediates the action of Sema3F.

As for dendrites, Sema3F-induced growth cone collapse was not prevented by either SQ 22,536 or KT 5720 (Fig. 8), but was overcome by forskolin and 8-Br-cAMP (Fig. 9). These results demonstrate that cAMP/PKA signaling has totally different roles in the response of axons and dendrites to Sema3F.

DISCUSSION

Dentate granule cells extend their axons and dendrites in opposing directions; the axons extend to the hilar region, and dendrites extend to the molecular layer (1, 2). Because this polarity disappears in dissociated cultures, environmental factors present in the dentate gyrus are crucial for neurite polarization (3). Many studies have investigated neuritogenesis and neurite maturation of dentate granule cells, but most of them have focused only on the axons (3, 8, 27, 31, 34, 35, 57–59), and much less attention has been paid to dendrites. To understand neurite polarity, it is essential to monitor the behavior of axons and dendrites simultaneously. As a first step to this end, in this work, we used isolated dentate granule cells, a simplified experimental system that allowed us to trace developing axons and dendrites of the same cells without interruption by neurites of other nearby cells. We have shown that both axons and dendrites respond to Sema3F and glutamate with growth cone collapse, but that cAMP signaling is differentially involved.

cAMP Mediates Sema3F-induced Axonal Collapse—Very little is known about the Sema3F signaling cascade. We have presented several lines of evidence concerning Sema3F and axonal collapse of dentate granule cells: (i) Sema3F increased cAMP levels in axonal growth cones; (ii) Sema3F-induced collapse was inhibited by blockade of cAMP signaling; (iii) cAMP stimulation alone could induce growth cone collapse;

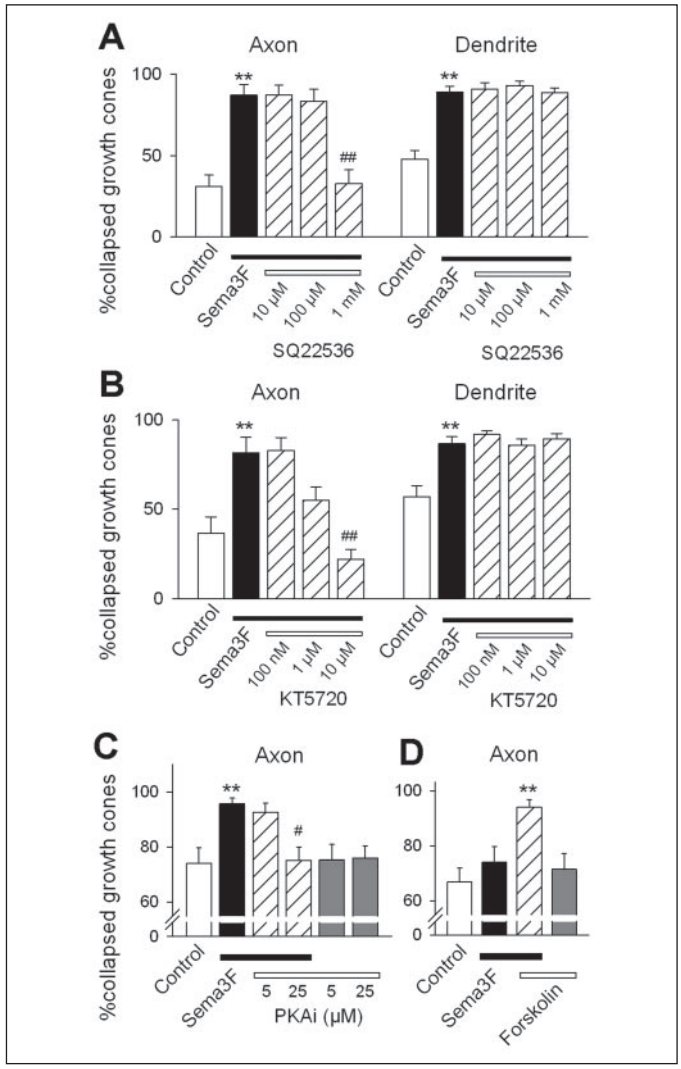

FIGURE 8. **cAMP signaling is required for Sema3F-induced growth cone collapse of axons, but not of dendrites.** *A–C*, Sema3F-induced growth cone collapse was evaluated 10 min after co-treatment with SQ 22,536, KT 5720, and myristoylated PKI peptide (*PKAi*), respectively. Cultures were pretreated with SQ 22,536, KT 5720, and PKI for 30, 40, and 60 min, respectively, and exposed to Sema3F for 10 min in the presence of these drugs and peptide (*hatched bars*). Data represent means ± S.E. of 19–24 neurons from three independent experiments (*A*), 18–29 neurons from three experiments (*B*), and 38–40 neurons from four experiments (*C*). *, $p < 0.05$ *versus* control; **, $p < 0.01$ *versus* control; #, $p < 0.05$ *versus* Sema3F; ##, $p < 0.01$ *versus* Sema3F (Tukey's test after ANOVA). *D*, forskolin and Sema3F had a synergic effect on axonal growth cone collapse. Granule cells were treated for 10 min with subthreshold doses of forskolin (3 μM; *gray bar*), Sema3F (1:128 dilution; *black bar*), or both (*hatched bar*). Either alone did not induce growth cone collapses, but their combination readily did. Data represent means ± S.E. of 38–40 neurons from four independent experiments. **, $p < 0.01$ *versus* control (Tukey's test after ANOVA).

and (iv) the actions of Sema3F and cAMP were synergic and occlusive. We thus believe that cAMP directly mediates Sema3F-induced growth cone collapse.

cAMP has been reported to modulate the response of growth cones in various types of neurons to different guidance molecules. In most cases, the contribution of cAMP is indirect; cAMP regulates (rather than directly brings about) a collapse response. Exceptions are netrin-1 and sonic hedgehog: netrin-1 increases cAMP levels to attract *Xenopus* retinal growth cones, an effect that is prevented by laminin-1 (60), and sonic hedgehog reduces cAMP levels and thereby suppresses neurite outgrowth in chick retinal ganglion cells (44). Our observation is therefore the first evidence that cAMP is directly involved in semaphorin signaling. Growth cone collapse induced by Sema3A, the most studied

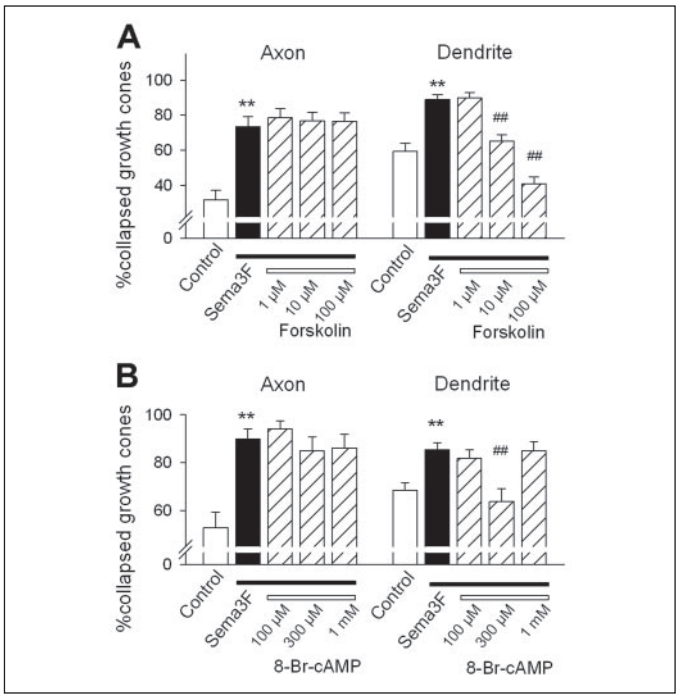

FIGURE 9. **Activation of cAMP signaling antagonizes Sema3F-induced growth cone collapse of dendrites, but not of axons.** Sema3F-induced growth cone collapse were evaluated 10 min after co-treatment with forskolin (*A*) or 8-Br-cAMP (*B*). Cultures were pretreated with forskolin and 8-Br-cAMP for 20 and 30 min, respectively, and exposed to Sema3F for 10 min in the presence of these drugs (*hatched bars*). Data represent means ± S.E. of 36–50 neurons from six independent experiments (*A*) and 23–38 neurons from four independent experiments (*B*). **, $p < 0.01$ *versus* control; ##, $p < 0.01$ *versus* Sema3F (Tukey's test after ANOVA).

member of the class 3 semaphorin family, is unlikely to undergo cAMP modulation in *Xenopus* spinal neurons (4) or *Xenopus* retinal ganglion cells (7); but in chick dorsal root ganglions, cAMP analogs inhibit Sema3A-induced axonal collapse (6). Therefore, the cAMP involvement in semaphorin signaling appears to differ among various types of neurons. We have demonstrated here that, in identical cells, it differs even between axons and dendrites.

We previously demonstrated that the axons of granule cells transplanted ectopically close to host CA1 slices do not intrude into the host slices, but they do intrude and even make functional synapses with CA1 neurons if cAMP signaling is blocked (8). Because *Sema3F* mRNA is present in the CA1 stratum pyramidale (32, 33), this ectopic synaptogenesis may be explained by the fact that inhibition of cAMP singling prevents Sema3F-induced collapse of granule cell axons.

cAMP Prevents Sema3F-induced Dendritic Collapse—The hippocampal formation including the dentate gyrus expresses *Sema3F* mRNA throughout a lifetime (32, 33), although its protein level has not been determined. Sema3F acts as a potent repellent against mossy fiber growth (31, 34) and may contribute to stereotyped pruning of mossy fibers in the hippocampus (35). We have shown that the axons and dendrites of granule cells are similarly responsive to Sema3F. This is in marked contrast with the case of Sema3A. Sema3A was characterized as a chemorepellent for the axons of cortical pyramidal neurons (61), but it was later shown to attract the apical dendrites toward the cortical superficial layer, where Sema3A is expressed at higher levels compared with the deep layers (62, 63). Soluble guanylyl cyclase is asymmetrically distributed in cortical pyramidal cells, making a vertical gradient of cGMP, with a high concentration in apical dendrites and a low concentration in axons (62). This asymmetric distribution probably contributes to the axodendritic polarization of a cortical pyramidal neuron. On the other hand, we found that Sema3F collapsed the axons and dendrites of dentate granule cells with almost equal potency and that both neurites expressed adenylyl cyclase to a similar extent and exhibited an increase in cAMP levels in response to forskolin. Nonetheless, Sema3F induced a cAMP increase only in axons. Moreover, cAMP stimulation led to opposite results, *i.e.* a decrease in axonal growth cones and an increase in dendritic growth cones.

In dendrites, cAMP may modulate (rather than directly mediate) Sema3F-induced collapse of growth cones because Sema3F did not increase or decrease cAMP levels at all. It is also therefore possible that the cAMP and Sema3F cascades work in a completely independent manner. In this study, we could not illuminate the mechanisms responsible for this differential cAMP regulation, but investigation is now underway to examine how Ca^{2+} dynamics in growth cones differ between axons and dendrites because type 1 adenylyl cyclase is activated by Ca^{2+}/calmodulin (64). Terman and Kolodkin (65) have shown that Nervy, a member of the myeloid translocation gene family of PKA-anchoring proteins, links PKA to plexin A and regulates semaphorin signaling. It is possible that, in dentate granule cells, PKA-anchoring proteins couple cAMP signaling to Sema3F and that the different responsiveness to cAMP between axons and dendrites could be explained by localization of PKA-anchoring proteins.

Fujioka *et al.* (66) have recently indicated that activation of the cAMP cascade increases the length and branch point number of dendrites of developing granule cells *in vivo* and *in vitro* and that this is likely to depend on phosphorylation of the cAMP-response element-binding protein. Although neurite elongation and branching are not necessarily associated with growth cone dynamics, their results are in remarkable agreement with our observations of cAMP-induced increases in dendritic growth cones.

Glutamate as a Repellant against Granule Cell Growth Cones—Glutamate is an excitatory neurotransmitter used in transmission of granule cell synapses (16–21). Neurogenesis of granule cells persists throughout life (22–24), so neurite guidance of granule cells also continues to occur throughout life. Glutamate is likely to spillover from synaptic clefts (26). Such glutamate leakage from pre-existing synapses may affect pathfinding by immature granule cells. Our finding that glutamate induces growth cone collapse suggests that growing axons and dendrites are repelled by spillover of glutamate. This may help newly formed synapses to avoid overlapping with already active, pre-existing synapses, diminishing a functional redundancy in the dentate circuit.

Glutamate-induced dendritic collapse was mediated by group I/II metabotropic glutamate receptors and rescued by activation of cAMP signaling. The protection by cAMP was also observed against Sema3F. cAMP possibly protects dendritic growth cones from any external repellents. On the other hand, it is intriguing that cAMP-induced axonal collapse (Fig. 3) did not take place when group I/II metabotropic glutamate receptors were activated (Fig. 1*C*). Group I/II metabotropic glutamate receptor activity may prevent axonal collapse induced by a reduction of cAMP.

Conclusion—In summary, we have illustrated the differential cAMP regulation of axonal and dendritic outgrowth of dentate granule cells. Although further investigations must elucidate the molecular basis in detail, this work has provided an important framework to understand the axodendritic difference in neurite growth, *i.e.* cAMP may be a critical factor in shaping the axodendritic polarity of dentate granule cells.

Acknowledgments—We thank Dr. Atsushi Tamada for providing Sema3F-Myc cDNA and Dr. Junken Aoki for anti-Myc antibody. We are also grateful to Drs. Maki K. Yamada, Ryuta Koyama, and Jeong-Ah Kim for technical support and daily discussions and to Shizu Ohba for careful data shuffling to attain blind experiments.

REFERENCES

1. Desmond, N. L., and Levy, W. B. (1982) *J. Comp. Neurol.* **212,** 131–145
2. Claiborne, B. J., Amaral, D. G., and Cowan, W. M. (1990) *J. Comp. Neurol.* **302,** 206–219
3. Kim, J.-A., Koyama, R., Yamada, R. X., Yamada, M. K., Nishiyama, N., Matsuki, N., and Ikegaya, Y. (2004) *Cereb. Cortex* **14,** 1358–1369
4. Song, H., Ming, G., He, Z., Lehmann, M., McKerracher, L., Tessier-Lavigne, M., and Poo, M. (1998) *Science* **281,** 1515–1518
5. Song, H. J., Ming, G. L., and Poo, M. M. (1997) *Nature* **388,** 275–279
6. Dontchev, V. D., and Letourneau, P. C. (2002) *J. Neurosci.* **22,** 6659–6669
7. Campbell, D. S., Regan, A. G., Lopez, J. S., Tannahill, D., Harris, W. A., and Holt, C. E. (2001) *J. Neurosci.* **21,** 8538–8547
8. Mizuhashi, S., Nishiyama, N., Matsuki, N., and Ikegaya, Y. (2001) *J. Neurosci.* **21,** 6181–6194
9. McKinney, R. A., Capogna, M., Durr, R., Gahwiler, B. H., and Thompson, S. M. (1999) *Nat. Neurosci.* **2,** 44–49
10. Wong, W. T., and Wong, R. O. (2000) *Curr. Opin. Neurobiol.* **10,** 118–124
11. Fischer, M., Kaech, S., Wagner, U., Brinkhaus, H., and Matus, A. (2000) *Nat. Neurosci.* **3,** 887–894
12. Chang, S., and De Camilli, P. (2001) *Nat. Neurosci.* **4,** 787–793
13. Tashiro, A., Dunaevsky, A., Blazeski, R., Mason, C. A., and Yuste, R. (2003) *Neuron* **38,** 773–784
14. Lipton, S. A., and Kater, S. B. (1989) *Trends Neurosci.* **12,** 265–270
15. Zheng, J. Q., Wan, J. J., and Poo, M. M. (1996) *J. Neurosci.* **16,** 1140–1149
16. Storm-Mathisen, J. (1981) *Adv. Biochem. Psychopharmacol.* **27,** 43–55
17. Bekenstein, J. W., Bennett, J. P., Jr., Wooten, G. F., and Lothman, E. W. (1990) *Brain Res.* **514,** 334–342
18. Terrian, D. M., Gannon, R. L., and Rea, M. A. (1990) *Neurochem. Res.* **15,** 1–5
19. Sandler, R., and Smith, A. D. (1991) *J. Comp. Neurol.* **303,** 177–192
20. Conner-Kerr, T. A., Simmons, D. R., Peterson, G. M., and Terrian, D. M. (1993) *J. Neurochem.* **61,** 627–636
21. Jones, R. S. (1994) *Hippocampus* **4,** 335–353
22. Altman, J., and Das, G. D. (1965) *J. Comp. Neurol.* **124,** 319–335
23. Kaplan, M. S., and Hinds, J. W. (1977) *Science* **197,** 1092–1094
24. Kuhn, H. G., Dickinson-Anson, H., and Gage, F. H. (1996) *J. Neurosci.* **16,** 2027–2033
25. van Praag, H., Schinder, A. F., Christie, B. R., Toni, N., Palmer, T. D., and Gage, F. H. (2002) *Nature* **415,** 1030–1034
26. Kullmann, D. M., and Asztely, F. (1998) *Trends Neurosci.* **21,** 8–14
27. Koyama, R., Yamada, M. K., Nishiyama, N., Matsuki, N., and Ikegaya, Y. (2002) *J. Physiol.* (*Lond.*) **539,** 157–162
28. Tessier-Lavigne, M., and Goodman, C. S. (1996) *Science* **274,** 1123–1133
29. Takahashi, T., Fournier, A., Nakamura, F., Wang, L. H., Murakami, Y., Kalb, R. G., Fujisawa, H., and Strittmatter, S. M. (1999) *Cell* **99,** 59–69
30. Giger, R. J., Urquhart, E. R., Gillespie, S. K., Levengood, D. V., Ginty, D. D., and Kolodkin, A. L. (1998) *Neuron* **21,** 1079–1092
31. Cheng, H. J., Bagri, A., Yaron, A., Stein, E., Pleasure, S. J., and Tessier-Lavigne, M. (2001) *Neuron* **32,** 249–263
32. Chedotal, A., Del Rio, J. A., Ruiz, M., He, Z., Borrell, V., de Castro, F., Ezan, F., Goodman, C. S., Tessier-Lavigne, M., Sotelo, C., and Soriano, E. (1998) *Development* (*Camb.*) **125,** 4313–4323
33. Barnes, G., Puranam, R. S., Luo, Y., and McNamara, J. O. (2003) *Hippocampus* **13,** 1–20
34. Chen, H., Bagri, A., Zupicich, J. A., Zou, Y., Stoeckli, E., Pleasure, S. J., Lowenstein, D. H., Skarnes, W. C., Chedotal, A., and Tessier-Lavigne, M. (2000) *Neuron* **25,** 43–56
35. Bagri, A., Cheng, H. J., Yaron, A., Pleasure, S. J., and Tessier-Lavigne, M. (2003) *Cell* **113,** 285–299
36. Sahay, A., Molliver, M. E., Ginty, D. D., and Kolodkin, A. L. (2003) *J. Neurosci.* **23,** 6671–6680
37. Baba, A., Yamada, M. K., Nishiyama, N., Matsuki, N., and Ikegaya, Y. (2002) *J. Neurocytol.* **31,** 41–48
38. Baba, A., Yasui, T., Fujisawa, S., Yamada, R. X., Yamada, M. K., Nishiyama, N., Matsuki, N., and Ikegaya, Y. (2003) *J. Neurosci.* **23,** 7737–7741
39. Dent, E. W., and Kalil, K. (2001) *J. Neurosci.* **21,** 9757–9769
40. Craig, A. M., and Banker, G. (1994) *Annu. Rev. Neurosci.* **17,** 267–310
41. Lamoureux, P., Ruthel, G., Buxbaum, R. E., and Heidemann, S. R. (2002) *J. Cell Biol.* **159,** 499–508
42. Luo, Y., Raible, D., and Raper, J. A. (1993) *Cell* **75,** 217–227
43. Fan, J., Mansfield, S. G., Redmond, T., Gordon-Weeks, P. R., and Raper, J. A. (1993) *J. Cell Biol.* **121,** 867–878
44. Trousse, F., Marti, E., Gruss, P., Torres, M., and Bovolenta, P. (2001) *Development* (*Camb.*) **128,** 3927–3936
45. Yamaguchi, N., Takanezawa, Y., Koizumi, H., Umezu-Goto, M., Aoki, J., and Arai, H. (2004) *FEBS Lett.* **566,** 71–76
46. Koyama, R., Yamada, M. K., Nishiyama, N., Matsuki, N., and Ikegaya, Y. (2004) *Dev. Biol.* **267,** 29–42
47. Pin, J. P., and Duvoisin, R. (1995) *Neuropharmacology* **34,** 1–26
48. Hei, Y. J., MacDonell, K. L., McNeill, J. H., and Diamond, J. (1991) *Mol. Pharmacol.* **39,** 233–238
49. Fabbri, E., Brighenti, L., and Ottolenghi, C. (1991) *J. Enzyme Inhib.* **5,** 87–98
50. Huang, Y. Y., Martin, K. C., and Kandel, E. R. (2000) *J. Neurosci.* **20,** 6317–6325
51. Davies, S. P., Reddy, H., Caivano, M., and Cohen, P. (2000) *Biochem. J.* **351,** 95–105
52. Metzger, H., and Lindner, E. (1981) *Arzneim-Forsch* **31,** 1248–1250
53. Schaefer, M. L., Wong, S. T., Wozniak, D. F., Muglia, L. M., Liauw, J. A., Zhuo, M., Nardi, A., Hartman, R. E., Vogt, S. K., Luedke, C. E., Storm, D. R., and Muglia, L. J. (2000) *J. Neurosci.* **20,** 4809–4820
54. Mons, N., Guillou, J. L., Decorte, L., and Jaffard, R. (2003) *Neurobiol. Learn. Mem.* **79,** 226–235
55. Villacres, E. C., Wong, S. T., Chavkin, C., and Storm, D. R. (1998) *J. Neurosci.* **18,** 3186–3194
56. Harris, T. E., Persaud, S. J., and Jones, P. M. (1997) *Biochem. Biophys. Res. Commun.* **232,** 648–651
57. Grimpe, B., Dong, S., Doller, C., Temple, K., Malouf, A. T., and Silver, J. (2002) *J. Neurosci.* **22,** 3144–3160
58. Butler, C. D., Schnetz, S. A., Yu, E. Y., Davis, J. B., Temple, K., Silver, J., and Malouf, A. T. (2004) *J. Neurosci.* **24,** 462–473
59. Koyama, R., and Ikegaya, Y. (2004) *Curr. Neurovasc. Res.* **1,** 3–10
60. Hopker, V. H., Shewan, D., Tessier-Lavigne, M., Poo, M., and Holt, C. (1999) *Nature* **401,** 69–73
61. Polleux, F., Giger, R. J., Ginty, D. D., Kolodkin, A. L., and Ghosh, A. (1998) *Science* **282,** 1904–1906
62. Polleux, F., Morrow, T., and Ghosh, A. (2000) *Nature* **404,** 567–573
63. Sasaki, Y., Cheng, C., Uchida, Y., Nakajima, O., Ohshima, T., Yagi, T., Taniguchi, M., Nakayama, T., Kishida, R., Kudo, Y., Ohno, S., Nakamura, F., and Goshima, Y. (2002) *Neuron* **35,** 907–920
64. Defer, N., Best-Belpomme, M., and Hanoune, J. (2000) *Am. J. Physiol.* **279,** F400–F416
65. Terman, J. R., and Kolodkin, A. L. (2004) *Science* **303,** 1204–1207
66. Fujioka, T., Fujioka, A., and Duman, R. S. (2004) *J. Neurosci.* **24,** 319–328